

1.33 The Two-/Three-Dimensional HPLC Mapping Method for the Identification of *N*-Glycan Structures

N. Takahashi, H. Yagi, and K. Kato, Nagoya City University, Nagoya, Japan
© 2007 Elsevier Ltd. All rights reserved.

1.33.1 Introduction: HPLC Mapping Method	1
1.33.2 Principles of Two-/Three-Dimensional HPLC Mapping Method	2
1.33.2.1 Releasing of <i>N</i> -Glycans	2
1.33.2.1.1 Glycoamidase A	2
1.33.2.1.2 Other glycoamidases	3
1.33.2.2 Pyridylation of Oligosaccharides	3
1.33.2.3 Code Numbers for the PA-Glycans	3
1.33.2.4 Glucose Units	4
1.33.2.5 The Two-/Three-Dimensional HPLC Mapping Method	4
1.33.2.5.1 Two-dimensional mapping technique for neutral PA-glycans	4
1.33.2.5.2 Extension to 3-D mapping technique for sialyl PA-glycans	5
1.33.3 Application of HPLC Mapping Method	7
1.33.3.1 A New Concept, Unit Contribution	7
1.33.3.1.1 Introduction of a unit contribution	7
1.33.3.1.2 Application of the UC value diagrams	8
1.33.3.2 Identification of Molecular Species and Linkages of Sialyl Oligosaccharides	11
1.33.3.3 <i>N</i> -Glycosylation Profiles in Cell and Tissue Levels	12
1.33.3.4 Development of HPLC Map for Sulfated Oligosaccharides	13
1.33.3.5 A Web Application, GALAXY	14
1.33.3.6 A New Idea of HPLC Map Related to Microheterogeneity of <i>N</i> -Glycans	14
1.33.3.6.1 Application of parallelogram method to validate <i>N</i> -glycan structures on the 2-D map	15
1.33.3.6.2 Visual presentation of the <i>N</i> -glycan microheterogeneity	15
1.33.4 Summary	16

1.33.1 Introduction: HPLC Mapping Method

s0005

Structural elucidation of carbohydrate chains is of fundamental importance in studies of glycoconjugates. Typical methods for structural determination employ a variety of techniques such as methylation, periodate oxidation and enzymatic digestion, as well as nuclear magnetic resonance (NMR) and mass spectroscopy. Recent development in chromatographic techniques allows a new approach to the determination of the carbohydrate structure with or without derivatization of the oligosaccharides. The separation and identification of oligosaccharide derivatives on extremely small scales were carried out by high-performance liquid chromatography (HPLC) procedures. Typical examples of fine separation are obtained in the IgG oligosaccharides. There are very similar structures of even the same molecular weight which can be completely separated by reverse-phase column chromatography. There are many different methods for analysis of oligosaccharides, especially those associated with glycoproteins or glycolipids. Correlation of elution volume and structure has been quite well established for the amino acid analyzer. In our approach, liquid chromatography is carried out in two different column-solvent combinations, allowing the two coordinates to be related to the structure of a given oligosaccharide (two-dimensional (2-D) mapping) We will briefly explain the method we developed: the 2/3-D HPLC mapping method using pyridylaminated oligosaccharides (PA-oligosaccharides), developed for the structural determination of asparagine-linked oligosaccharides (*N*-glycans) in glycoproteins.

p0005

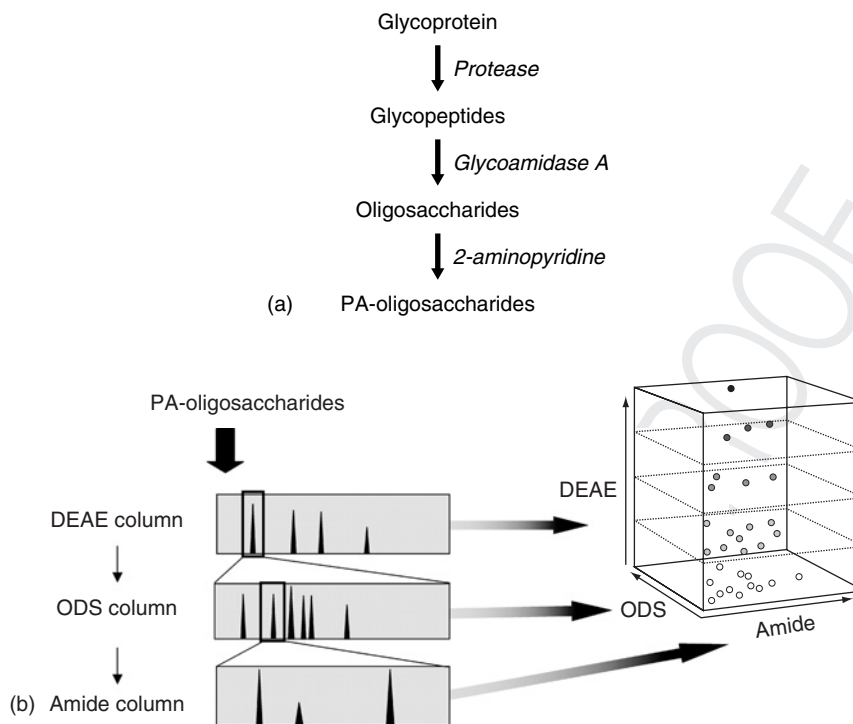


Figure 1 Schemes of preparation of (a) PA-oligosaccharides and (b) structural analysis by HPLC mapping method.

f0005

The *N*-glycans are first released from the protein portion by digestion with glycoamidase A, and the reducing ends of the oligosaccharides are fluorescently labeled with 2-aminopyridine (Figure 1a). These PA-glycans are then separated by HPLC using three different columns sequentially. Based on the elution times on the three kinds of HPLC columns, the structures of the separated PA-glycans are estimated by comparing their elution times with the times of the known reference *N*-glycans plotted on the HPLC map (Figure 1b). Then, the sample PA-glycan and one or more of the candidate reference PA-glycans are co-injected into two HPLC columns to confirm its identity (total coincidence of elution position). In addition, the sample PA-glycan is digested with several glycosidases, then the changes in the elution positions are again compared with those of the reference *N*-glycans.

p0010

In order to familiarize the reader with the actual application of these methods to *N*-glycan analysis, the authors describe several examples from our published results. During the process, it will be demonstrated that the oligosaccharides of different structure, even very closely related ones, can be separated by this 3-D map approach.

p0015

At least 1 mg of the sample glycoprotein is required by the technique as starting material, although only picomole or femtomole levels of the PA-oligosaccharides are necessary for one run of HPLC analysis.

p0020

The method is useful not only as an analytical procedure for *N*-glycan structures, but also as a means for isolation of samples for NMR spectroscopy or MS spectrometry.

p0025

1.33.2 Principles of Two-/Three-Dimensional HPLC Mapping Method

s0010

1.33.2.1 Releasing of *N*-Glycans

s0015

1.33.2.1.1 Glycoamidase A

s0020

Hydrazinolysis has been the most commonly used method to release *N*-linked oligosaccharides from glycoproteins. Hydrazinolysis, however, removes *N*-acyl groups from the oligosaccharides, and is accompanied by many undesirable side reactions. Therefore we usually release oligosaccharide moiety from the peptide portions by using glycoamidase A (EC 3.5.1.52), which N. Takahashi discovered from almond emulsin in 1977¹. The enzyme purification methods or the detailed specificities were published elsewhere.^{2,3} The mode of action of the enzyme is shown in Figure 2. Reaction [1] is catalyzed by the enzyme, and reaction [2] proceeds nonenzymatically. The resulting products of the reactions are a carbohydrate chain with chitobiose at the reducing end, a carbohydrate-free peptide containing Asp at

p0030

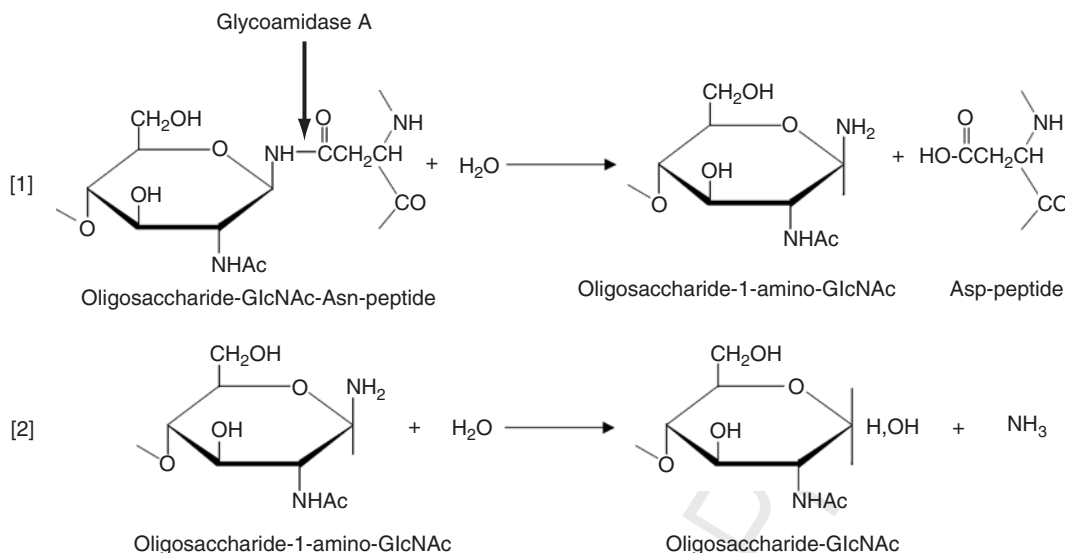


Figure 2 Reaction mechanism of glycoamidase A.

f0010

the former glycosylation site, and ammonia. This enzyme was named glycoamidase because its cleavage site is acid-amide linkage at the asparagine residue, indicating that the enzyme is not a glycosidase. All *N*-linked oligosaccharides so far analyzed and reported here were released from the glycopeptides by the glycoamidase A digestion. Glycoamidase A can successfully release *N*-linked oligosaccharides from neutral, sialylated, sulfated, or phosphorylated glycopeptides, and most importantly, even when the GlcNAc directly attached to Asn is $\alpha(1-3)$ fucosylated, on which the glycoamidase from *Chryseobacterium meningosepticum* (*Flavobacterium meningosepticum*) fails to act, as explained below.

1.33.2.1.2 Other glycoamidases

Similar plant origin glycoamidase belong to (EC 3.5.1.52) was reported to exist in jack bean meal by Sugiyama *et al.*⁴ The optimum pH of the enzyme is 6.5. The enzyme can release *N*-glycans from small glycopeptides with three or more amino acid residues, but not from GlcNAc-Asn. Both high-mannose- and hybrid-type oligosaccharides of ovalbumin and both sialylated and nonsialylated biantennary sugar chains of fibrinogen can be released. Further analysis, to be published later, found glycoamidase activity with similar substrate specificities and confirmed its broad distribution in seeds or beans.

Several years after the discovery of glycoamidase A from almond, another similar enzyme discovered in the culture fluid of *Chryseobacterium meningosepticum* was also reported.^{5,6} This enzyme, however, cannot cleave common oligosaccharides in plant glycoproteins including an $\alpha(1,3)$ -linked fucose residue in the chitobiose core. Now this enzyme is available in three different commercial names, *N*-glycanase, *N*-glycosidase F, and peptide:*N*-glycosidase F (PNGase F).

1.33.2.2 Pyridylamination of Oligosaccharides

In order to induce fluorescence of the reducing oligosaccharide mixture, it is derivatized with 2-aminopyridine (Figure 3).⁷ S. Hase's improved PA-derivatization methods work well for sialylated oligosaccharides, as well as for neutral oligosaccharides. Because of its fluorescent nature, the sensitivity of detection of PA-oligosaccharides is in the subpicomol range. All experimental procedures from this section and the corresponding chromatographic conditions have been described in detail elsewhere.^{8,9}

1.33.2.3 Code Numbers for the PA-Glycans

The code number for a sialyl PA-glycan (Figure 4) consists of a set of several elements with the following meanings. For example, in '2A1-200.4' (Figure 4), 2A1 denotes disialyl-containing. The last numeral 1 is an arbitrarily assigned code number, and the number to the right of the hyphen (200.4) represents the neutral *N*-glycan code number, that is, the far left digit 2 means the number of antennae. The next digit '0' indicates the absence (or '1' the presence) of an

s0025

p0035

p0040

s0030

p0045

s0035

p0050

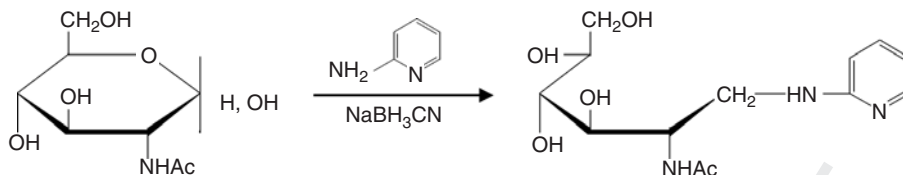


Figure 3 Reaction mechanism of oligosaccharides with 2-aminopyridine.

f0015

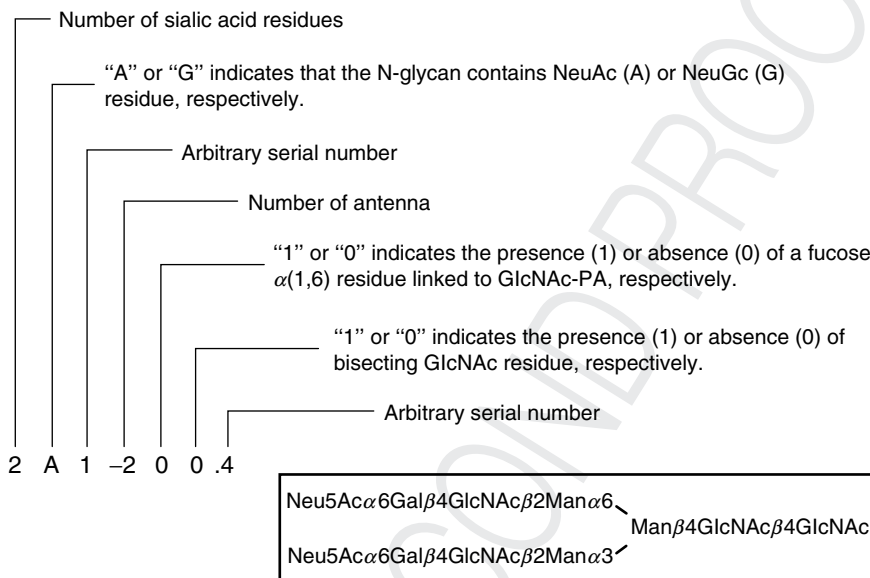


Figure 4 Code number.

f0020

α6-fucose residue bound to the reducing terminal *N*-acetylglucosamine residue. The third digit '0' indicates the absence (or '1' the presence) of bisecting GlcNAc residue. So, in the case of the absence of any other acidic group, the code numbers of standard oligosaccharides contain four or three elements, for example, 310.8 (triantennary complex type), or M5.1 (high-mannose type with five mannose residues).¹¹

The code numbers and structures of PA-oligosaccharides are recorded in the GALAXY website.¹⁰

p0055

1.33.2.4 Glucose Units

s0040

The elution time expressed in real time or actual volume varies depending on the individual column, its age, or the batches of buffers used. To alleviate day-to-day and column-to-column variations of elution positions, we adopt the concept of 'Glucose units (GU)' which is the representation of elution time, for example, 8.5, 10.3 (in min), as related to the elution position of homologous series of isomalto-oligosaccharides. In plotting the HPLC data on the 2-D or 3-D map, the GU are used. In practice, we calibrate every day both the octadecylsilica (ODS) and amide-silica columns with isomalto-oligosaccharide mixtures (dp=1–21). The GU (five, six, seven, etc.) indicate the degree of glucose polymerization. Next, a sample PA-oligosaccharide is applied to the same columns, and its elution position is proportionated by these reference oligosaccharides (Figure 5).

p0060

1.33.2.5 The Two-/Three-Dimensional HPLC Mapping Method

s0045

1.33.2.5.1 Two-dimensional mapping technique for neutral PA-glycans

s0050

In 1988, we proposed a 2-D sugar mapping method for the simple, reproducible, and sensitive analysis of the *N*-glycan structures.¹⁰ The structures of unknown oligosaccharides can be characterized from its elution positions on the map. The database for the sugar map was prepared with 113 authentic standard neutral oligosaccharides, 58 of

p0065

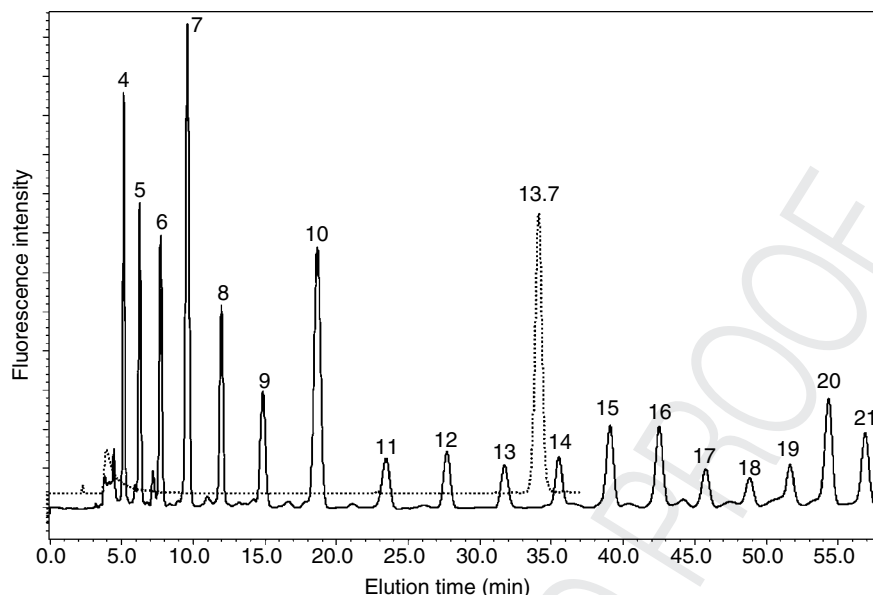


Figure 5 How to express elution times as a glucose unit (GU). The solid and dashed lines show the elution profiles of PA-derivatized isomalto-oligosaccharide mixture and sample PA-glycan, respectively. The ODS column was first calibrated with a commercial PA-derivatized isomalto-oligosaccharide mixture. Numbers (4, 5, 6, etc.) indicate the degree of α -1,6 glucose polymerization. The elution time of the sample compared with those of glucose oligomers and the GU of the sample were estimated for 13.7.

f0025

which have been confirmed by ^1H NMR spectroscopy. The 2-D mapping method involves four steps: (1) separation of oligosaccharide PA-derivatives by HPLC with an ODS-silica column, (2) analysis of the size of each separated oligosaccharide on an amide-silica column, (3) plotting of the elution position of a sample on the 2-D sugar map obtained for the reference oligosaccharides, and (4) structural estimation of the oligosaccharides by a combination of sequential exoglycosidase digestions.

Sometimes, a direct comparison of the coordinate values of the sample and the reference compound PA-oligosaccharides cannot give exact coincidence. In **Figure 6**, the elution positions of the sample obtained experimentally are 9.5 GU value on the ODS column [GU(ODS)] and 6.0 GU value on the amide column [GU(amide)], which represent (9.5, 6.5; wherever coordinates are cited in this chapter, they are always listed in the order of GU(ODS, amide)), for which there exist two candidate oligosaccharides, (9.6, 6.1) and (9.4, 5.9), with close values of coordinates. In such cases, coinjection with reference PA-oligosaccharide is the most reliable solution. However, glycosidase digestion methods, when applicable, are also very useful. Actually the elution positions of the two candidate oligosaccharides in **Figure 6** are very close, but after β -*N*-acetylhexosaminidase digestion, the elution positions of the resultant two oligosaccharides separate clearly. Then, after sequential digestion of β -galactosidase and again β -*N*-acetylhexosaminidase, the elution position of each reference oligosaccharide finally changes to the common trimannosyl core structure, by different pathways. In reality, each PA-glycan isolated on the ODS and amide-silica columns was digested by exoglycosidases (β -galactosidase and β -*N*-acetylhexosaminidase from jack bean) under the conditions described previously.¹²

p0070

We reported the 2-D mapping technique in 1988¹², and we were able to identify by 1995 many neutral *N*-glycan structures found in the various natural resources: urinary and recombinant erythropoietin 1988,¹⁴ porcine pancreatic Kallikrein 1988,¹⁵ human IgG subclass protein 1987,¹⁶ fibrinogen asahi 1989,¹⁷ taste-modifying protein miraculin 1990,¹⁸ human IgG3 subclass 1990,¹⁹ rice α -amylase 1990,²⁰ fibrinogen caracas II 1991,²¹ murine lymphocyte and lymphoma cells 1991,²² sycamore cells 1992,²³ nicotinic acetylcholine receptor 1992,²⁴ fibrinogen Lima 1992,²⁵ human urinary kallidinogenase 1993,²⁶ etc. The technique was later upgraded it to 3-D mapping in 1995.¹³

p0075

1.33.2.5.2 Extension to 3-D mapping technique for sialyl PA-glycans

s0055

The usefulness of the 2-D mapping technique depends on the numbers of reference compounds accurately analyzed and placed on the map. When the numbers of neutral oligosaccharides on the map reached more than 220, we thought

p0080

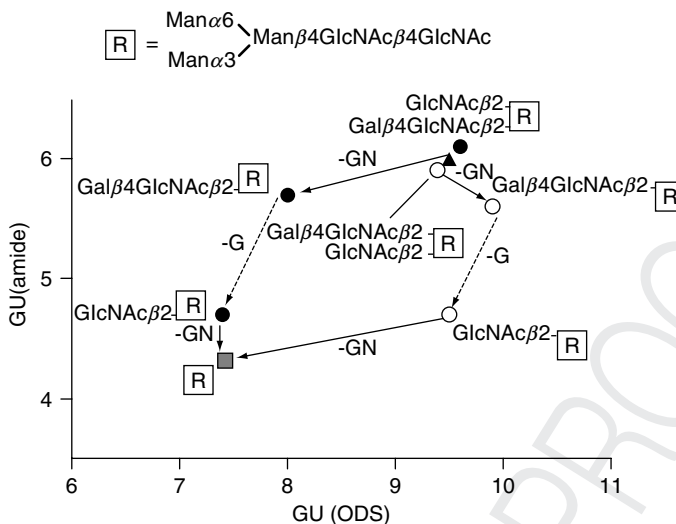


Figure 6 How to distinguish the most probable structure among candidate glycan structures. Trajectories for β -*N*-acetylhexosaminidase and β -galactosidase digestions were indicated by solid and dashed arrows, respectively. The elution positions of the two candidate glycans (200.2 and 200.3) are very close. After *N*-acetylhexosaminidase digestion, the resultant elution positions of the two candidate structures could be clearly distinguished from each other. Therefore, *N*-acetylhexosaminidase digestion of the sample may be the best way to determine its structure. G, galactose; GN, *N*-acetylhexosamine; ▲, sample glycans; ○, glycan (Code No. 200.2) and its digestion products; ●, glycan (Code No. 200.3) and its digestion products; ■, glycan (Code No. 000.1).

f0030

that it would be more useful to extend the technique to sialyl oligosaccharides, because the PA derivatization of sialyl oligosaccharides can be done efficiently. Thus, our 3-D map was born in 1995.⁹

In the first step, the PA-oligosaccharide mixture is separated on an anion-exchange column (TSKgel DEAE-5PW; 7.5 × 75mm, Tosoh) according to its sialic acid content, that is, neutral, monosialyl, disialyl, trisialyl, and tetrasialyl, etc. (Figure 7a). In the second step, each group mentioned above is injected separately onto a reverse-phase column (ShimPack HRC-ODS; 6 × 150mm, Shimadzu). The elution times are then recorded in GU, which become the *x*-coordinates. Separation on the ODS column depends on the fine structure of each oligosaccharide. Isomeric oligosaccharides, which cannot be differentiated by mass spectrometry easily, can be readily separated into several different structures on the ODS column. In the third step, each peak separated from the ODS column is applied to an amide-adsorption column (TSKgel Amide-80; 4.6 × 250mm Tosoh), and the elution times are recorded on the *y*-axis. Separation on the amide column depends mostly on the molecular size of each oligosaccharide. We found that the PA-derivatized sialyl oligosaccharides are also well separable on the same two HPLC columns (ODS and amide-silica) under completely the same elution conditions as used for the 2-D map for the neutral oligosaccharides.¹⁰ For each one of the groups separated by the DEAE column, a separate 2-D map is plotted. Repeating the whole process for each group of different sialylation levels, several layers of a 2-D map are obtained (Figure 7b). The elution positions from the ODS and amide columns provide a unique set of coordinate values for each PA-oligosaccharide. Plotting many sets of such HPLC data results in a 3-D map. The 3-D map (Figure 7d) can be graphically expressed either by a 2-D plot (Figure 7c), with different acidic groups for the different colors, for example, trisialyl oligosaccharide group is expressed by blue circle, in both Figures 7c and 7d)

p0085

It is important to point out that for each layer, the HPLC elution conditions used to obtain the *x*- and *y*-coordinates are all identical, so the coordinates can be transposed from layer to layer. However, if all the neutral and sialyl oligosaccharides are plotted on a single 2-D map, it becomes too complex and confusing. The use of the 3-D map is to avoid such confusion and complexity. There are no overlapping circles in each layer.

p0090

Once the 2/3-D maps are established, it is possible to characterize an unknown oligosaccharide by comparing with known reference compounds. This approach may be termed a library method. The underlying principle for the 2/3-D mapping method is simple. That is, different HPLC data mean different structures. If the unknown sample coincides with a known structure on the map, the sample may be identical to the known compound.

p0095

Since we reported the 3-D mapping technique in 1995,⁹ until 2005 we were able to determine the 3-D map coordinates of many neutral and sialyl *N*-glycan structures from natural resources: human coagulation factor X 1995,²⁷

p0100

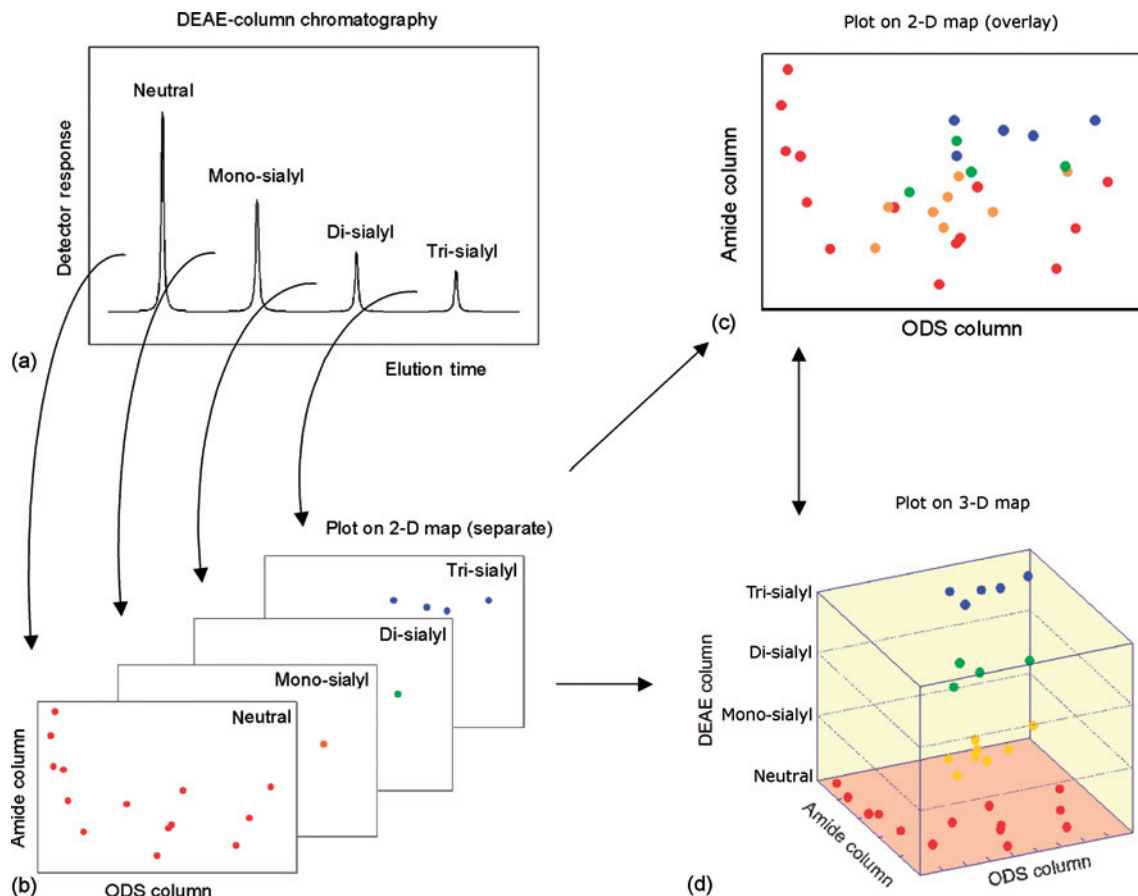


Figure 7 Transposition of the coordinates of the PA-glycans from a 2-D to a 3-D map. a, The PA-glycans are separated to neutral and sialyl glycans according to their sialic acid content on the first DEAE column. b, The coordinates were then plotted separately according to the sialic acid content. c, The coordinates can be transposed from layer to layer, so the coordinates of neutral and sialyl oligosaccharides are plotted all together on a 2-D map. d, The coordinates of the PA-glycans were plotted by the 3-D mapping technique. The lowest layer is that of the neutral oligosaccharides. Mono- and disialyl oligosaccharides are lined up on the z-axis according to their sialic acid content. These HPLC data of neutral and sialyl oligosaccharides derived from total glycoproteins in human serum.

f0035

human integrin $\alpha_5\beta_1$ 1996,²⁸ Bermuda grass antigen BG60 1996,²⁹ mutant IgG 1996,³⁰ outer membrane protein of *Chlamydia trachomatis* 1996,³¹ placental IgG 1996,³² IgGs from healthy control of various age 1997,³³ horseradish peroxidase 1998,³⁴ human IgG3 1998,³⁵ IgG from rheumatoid arthritis 1998 (review article by Routier *et al.*),³⁶ mouse soluble Fc γ receptor II 1998,³⁷ IgG from rheumatoid arthritis 1998 (an article by Mukofujiwara *et al.*),³⁸ fibrinogen niigata 1999,³⁹ neuropsin in *Trichoplusia ni* cells 1999,⁴⁰ osteopontin from human bone 2000,⁴¹ human transferrin in *T. ni* cells 2000,⁴² truncated IgG1 2000,⁴³ IgG cryoglobulin 2000,⁴⁴ pigeon egg white 2001,⁴⁵ specificity of mushroom lectin 2002,⁴⁶ recombinant human soluble Fc γ receptor III 2002,⁴⁷ IgG in patients 2002,⁴⁸ glycoprotein produced by baculovirus-infected insect cells 2003,⁴⁹ squid rhodopsin 2003,⁵⁰ and rabies virus 2005,⁵¹ etc.

1.33.3 Application of HPLC Mapping Method

1.33.3.1 A New Concept, Unit Contribution

1.33.3.1.1 Introduction of a unit contribution

We introduced a new concept, parameterization of unit contribution (UC).⁵²⁻⁵⁴ In this case, unit means each monosaccharide component at a specific position in a whole oligosaccharide. *N*-glycan structures can be arranged in

s0060

s0065

s0070

p0105

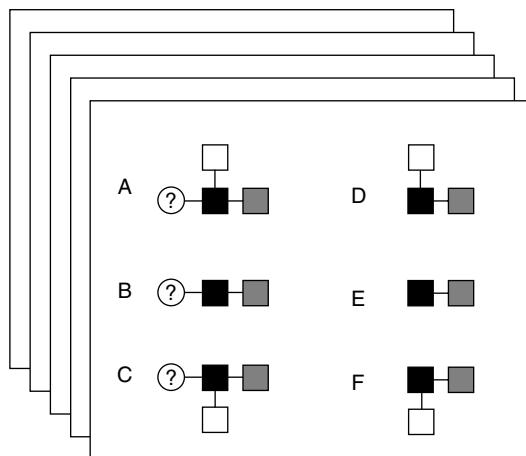


Figure 8 The principle of multiple regression.

f0040

a tree-like diagram, which spreads its branches on a trunk of a trimannosyl core structure. The basic assumption used in the parametrization is that the glucose unit of a given PA-oligosaccharide on an ODS or amide column can be represented by the total of the contributions of all its monosaccharide units. This approach is developed into a useful way to utilize UC values.

First, one can predict the coordinates of a PA-oligosaccharide for a given structure, even when it has not yet been reported. Second, the 2-D map helps predict the structure of oligosaccharides by eliminating possibilities which possess very different coordinates, and thus aids in further characterization for the exact structure.

p0110

Figure 8 explains the principle of multiple regression. Colored squares represent the same monosaccharide component. For example, to calculate the UCs of the white circle monosaccharide in the oligosaccharides A, B, and C, one has to take the difference with GU of the oligosaccharide on its right D, E, and F, respectively. The basic assumption used in our calculation was described previously.⁵⁵ The GU of a given PA-oligosaccharide on an ODS (or an amide-silica) column may be represented by the sum of the UCs of all component monosaccharides, as shown in the following equation:

p0115

$$\text{Elu}(i) = \text{UC}_1 \cdot x_1(i) + \text{UC}_2 \cdot x_2(i) + \dots + \text{UC}_n \cdot x_n(i)$$

where $\text{Elu}(i)$ is the observed elution time (expressed in GU) of compound number i , UC_1 – UC_n is elution time (GU) attributable to each component of the molecule, and $x_1(i)$ through $x_n(i)$ are independent variables for components 1 through n , which will be either 1 or 0, depending on the presence or absence of the component in the molecule. Calculation to obtain UC parameters was carried out by a linear multiple regression analysis with a commercial PC software (Statistica for Windows, StatSoft Inc., Tulsa, OK).

At present, a very good correlation was found between the observed and predicted elution time of 417 PA-glycans on an ODS column and on an amide-silica column based on the UC values of component monosaccharides.⁵⁴ These results clearly indicate that the application of the multiple regression calculation is a useful method for determining UC values (**Figure 9**).

p0120

1.33.3.1.2 Application of the UC value diagrams

s0075

Figure 10 shows the UC values calculated by multiple regression for high-mannose-type PA-oligosaccharides. These monosaccharides are all mannose residues, but due to the difference in their position and the linkage, they can be differentiated from each other. Using these values, we can calculate a completed 2-D map representation of all the possible high-mannose-type oligosaccharide structures derived from $\text{Glc}_1\text{Man}_9\text{GlcNAc}_2$. In other words, now we can estimate any structure as long as it is a high-mannose-type.

p0125

As an example of the usefulness of the UC value technique we tried the analysis of digestion pathway of high-mannose-type *N*-glycans with α -mannosidase from jack bean. We used the oligosaccharide $\text{Man}_9\text{GlcNAc}_2$ as

p0130

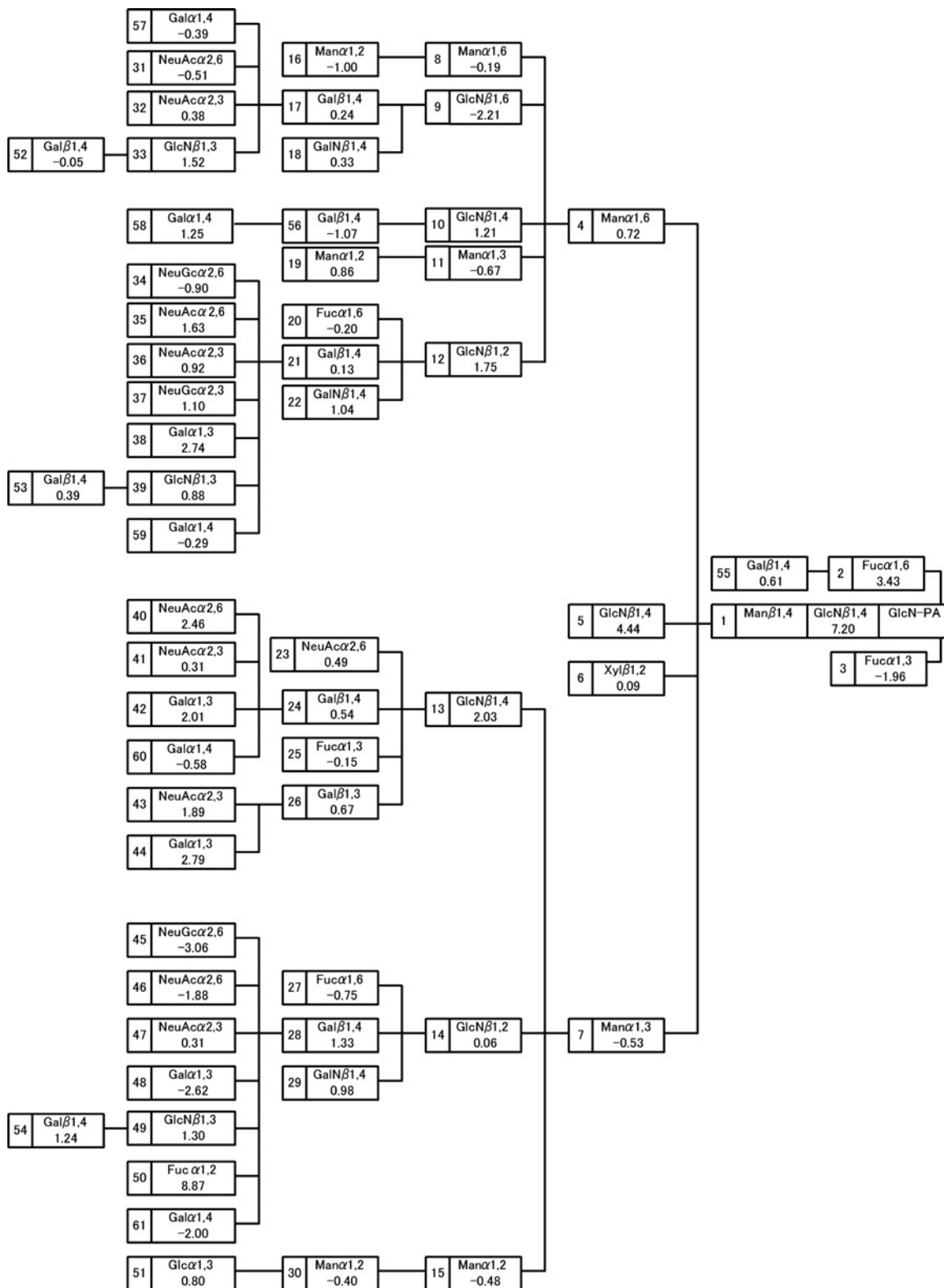


Figure 9 Diagram of the UC values, expressed in glucose units, for the elution positions of PA-glycans on an ODS columns. Component numbers are written on the left-hand side of each box; GlcN and GalN indicate GlcNAc and GalNAc, respectively.¹³

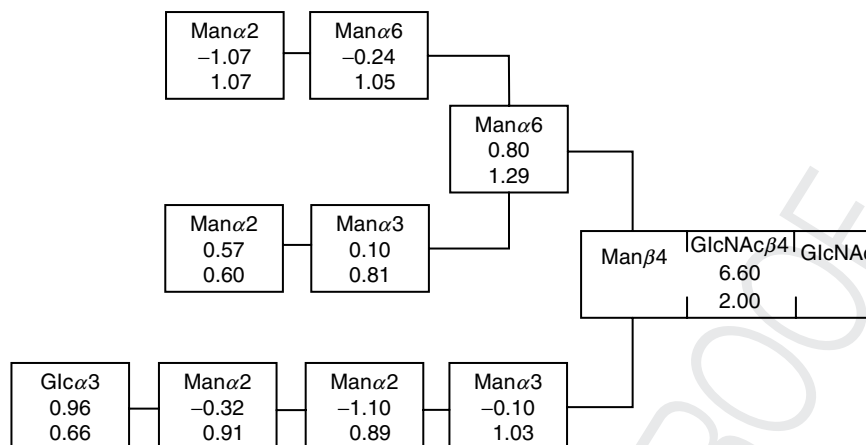


Figure 10 The UC values calculated by multiple regression for high-mannose-type PA-glycans. The upper and lower numbers in each box are the unit contribution values on the ODS and amide-silica columns, respectively.

f0050

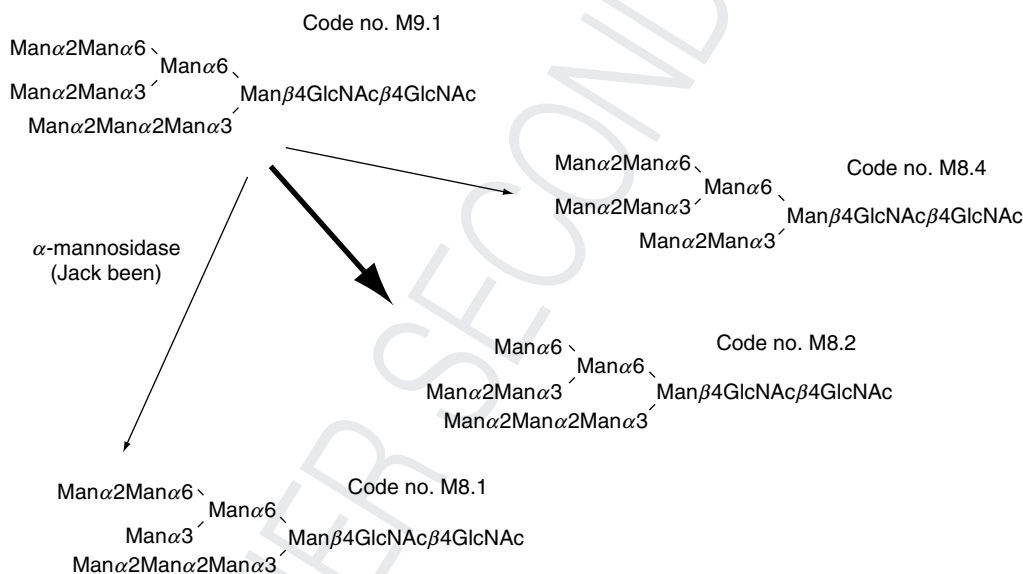


Figure 11 The terminal mannose residue on the $\text{Man}_\alpha 1\text{-}2\text{Man}_\alpha 1\text{-}6\text{Man}_\alpha 1\text{-}6\text{Man}$ arm is the first target of the jack bean α -mannosidase.

f0055

the starting substrate of the α -mannosidase. When this is digested with the enzyme, all possible intermediate oligosaccharides are readily calculated to be represented in the calculated 2-D map. For example, which mannose is the first target of the α -mannosidase is not clear from the beginning. There are three possible structures for $\text{Man}_8\text{GlcNAc}_2$, that is, M8.2, M8.1, and M8.4 (Figure 11). The GU(ODS)s of M8.1 (4.8) and M8.2 (6.4) were known data in the HPLC map. On the other hand, the GU(ODS) of M8.4 (5.7) was estimated by UC values. Actually, after the mannosidase digestion, the observed GU(ODS) of $\text{Man}_8\text{GlcNAc}_2$ was 6.5. Therefore, M8.1 with the GU of 4.8, and M8.4 with GU 5.7 can be eliminated. As a result, M8.2 with GU 6.4 is the most likely intermediate of the first-step degradation. Elucidation of other intermediates was carried out likewise. Thus, the pathway from $\text{Man}_9\text{GlcNAc}_2$ to $\text{Man}_1\text{GlcNAc}_2$ by jack bean α -mannosidase digestion was determined by the application of the calculated 2-D map (Figure 12).

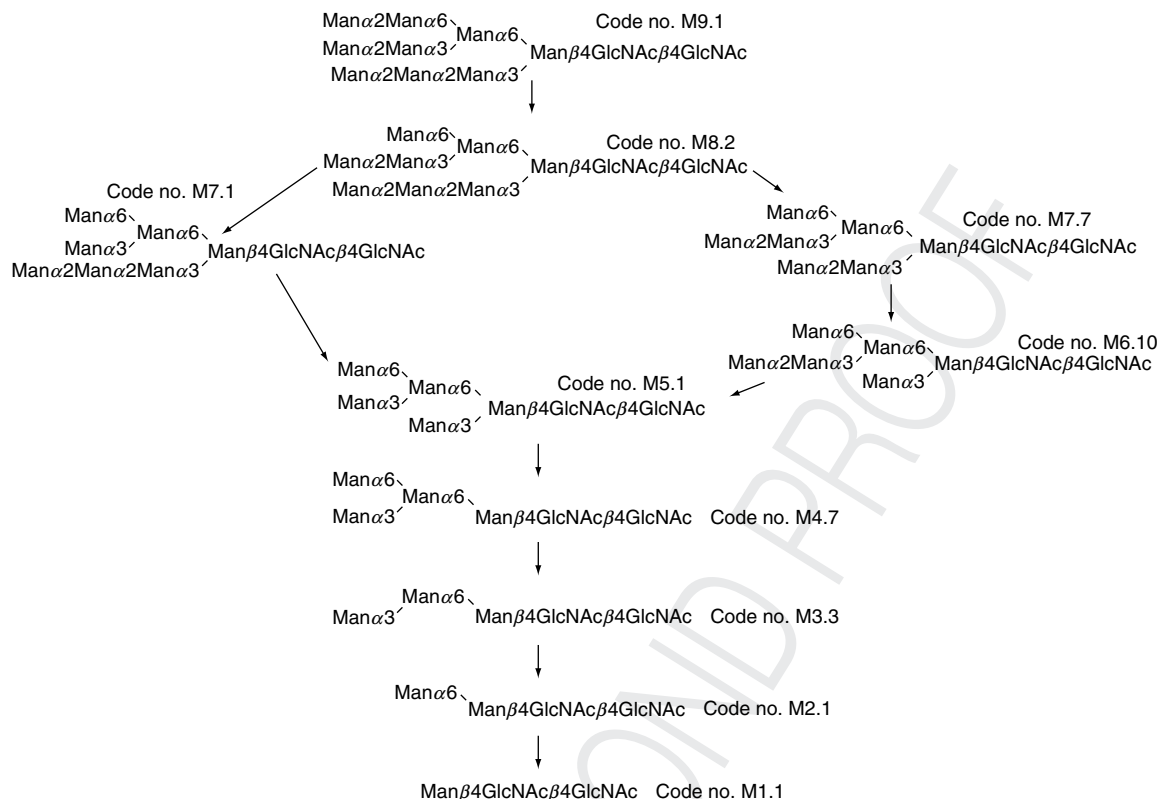


Figure 12 The pathway from $\text{Man}_9\text{GlcNAc}_2$ to $\text{Man}_7\text{GlcNAc}_2$ by jack bean α -mannosidase digestion was determined by the use of the calculated 2-D map. Owing to two different pathways, there existed two possible structures for each of the Man_7 and the Man_6 oligosaccharides.

1.33.3.2 Identification of Molecular Species and Linkages of Sialyl Oligosaccharides

In order to expand the database of sialyl oligosaccharides, we chose to prepare more sialyl oligosaccharides using an α 2,3-specific trans-sialidase from *Trypanosoma cruzi*, since it is difficult to obtain them from natural sources. From the pyridylamino derivatives of neutral and α 2,6-monosialylated biantennary oligosaccharides from human fibrinogen, five different sialyl biantennary oligosaccharides were obtained. A further 35 sialyl *N*-glycans were obtained from two different asialo-triantennary oligosaccharides from fetuin. The trans-sialidase transferred sialic acids effectively and indiscriminately to different galactosyl residues in the different positions on the substrates. Since the starting materials are neutral oligosaccharides of established structure, and the only α 2,3-sialyl residues are added to the nonreducing Gal terminal residues, the structures of these oligosaccharides could be identified unambiguously by using the 3-D mapping technique.¹³

The 3-D mapping technique is very useful for differentiating closely related α 2,3- and α 2,6-sialylated oligosaccharides. The results of the analyses of sialyl oligosaccharides have brought several surprises. For example, separation step by amide column on HPLC is often called as size fractionation. It means that PA-oligosaccharides are also fractionated on amide column by the size of samples. However, in the case of α 2,3-sialyl-containing oligosaccharides, α 2,3-sialyl residue contributes significantly to reduce the apparent size of the PA-oligosaccharide on an amide column, about 0.5 glucose unit on the *y*-axis. On the other hand, α 2,6-sialyl residue does not seem to contribute much to the apparent size ($<+0.1$ glucose unit on the *y*-axis per α 2,6-sialyl linkage)

An example in **Figure 13** shows HPLC data of the α 2,3- and/or α 2,6-sialylated biantennary PA-oligosaccharides.

Another advantage of the 3-D HPLC mapping technique for PA-oligosaccharides is its ability to differentiate between acidic groups such as Neu5Ac and Neu5Gc, although this differentiation is not so special a technique in other methods. **Figure 14** shows the HPLC data of biantennary complex-type glycans possessing Neu5Ac or Neu5Gc

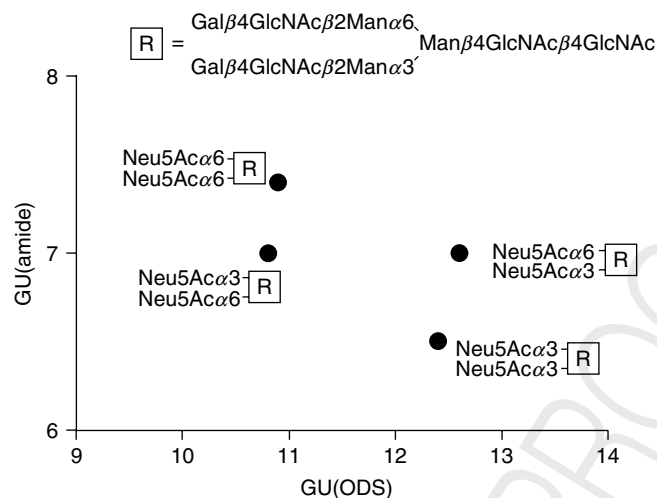


Figure 13 Identification of isomeric biantennary salooligosaccharides by HPLC map. The HPLC data of these isomeric glycans were different. f0065

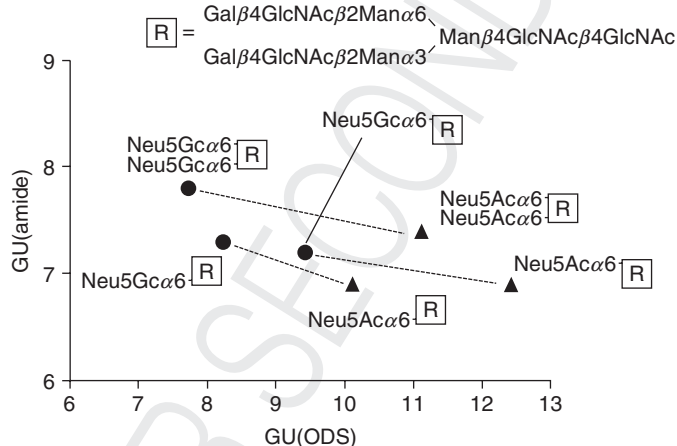


Figure 14 Comparison of the contribution of *N*-acetylneuraminic acid NeuAc_{2,6} and *N*-glycolylneuraminic acid NeuGc_{2,6} groups to the coordinates of the same biantennary oligosaccharides. Filled circles and filled triangles represent *N*-glycans possessing Neu5Gc and Neu5Ac residue(s), respectively. f0070

residues. The replacement of *N*-glycolyl neuraminic acid with *N*-acetyl neuraminic acid resulted in a larger elution time on the ODS column and an apparent reduced size on the amide column.

In this way, HPLC mapping method facilitates determination of isomeric *N*-glycans and molecular species sialic acids. p0155

1.33.3.3 *N*-Glycosylation Profiles in Cell and Tissue Levels s0085

Recently, the comprehensive structural determination and profiling of oligosaccharides in cell and tissue levels have been required, for which the HPLC mapping method proved to be a powerful tool. p0160

Figure 7d shows the HPLC map of neutral and sialyl oligosaccharides derived from total glycoproteins in human serum. Fourteen neutral, eight mono-sialyl, four di-sialyl, and five trisialyl oligosaccharides were isolated and identified by the HPLC mapping method.⁵⁰ In this method, *N*-glycans were released directly from 200 μl of human serum used as the starting material. Based on this experience, it would be easy to detect the change of the glycosylation profiles in human serum associated with various pathological stages. p0165

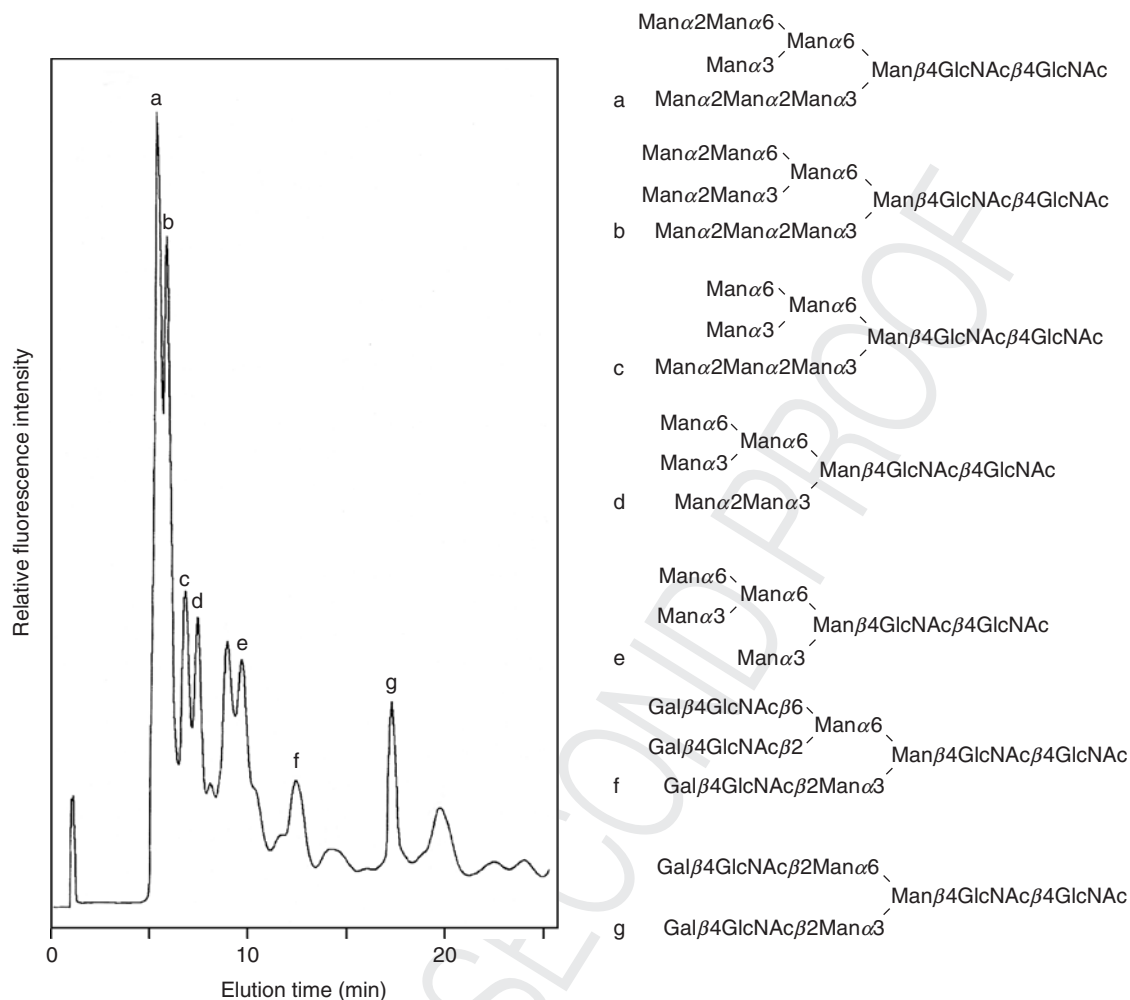


Figure 15 Glycosylation profiles on the ODS column derived from the surface glycoprotein fraction of *Chlamydia trachomatis*. f0075

In another example, **Figure 15** shows the glycosylation profiles derived from membrane protein fraction of *Chlamydia trachomatis* which is one of the most common causes of blindness and sexually transmitted diseases in humans. *C. trachomatis* expressed predominantly high-mannose-type oligosaccharides possessing 5, 6, 7, 8, and 9 mannose residues.^{50,155} These data indicated that the high-mannose-type oligosaccharides linked to membrane glycoproteins of *C. trachomatis* mediate attachment and infectivity of the organism to host cells. p0170

Thus, the multidimensional HPLC method is applicable to oligosaccharide profiling not only at molecular levels but also in cell, tissue, and organism levels. p0175

1.33.3.4 Development of HPLC Map for Sulfated Oligosaccharides s0090

It has been recently revealed that sulfated oligosaccharides on glycoproteins play important roles in biological functions, such as lymphocyte homing,⁵⁷ degradation of putative hormones,⁵⁸ and adhesion of neural cells.⁵⁹ It is necessary that the structures of these sulfated oligosaccharides are identified as a first step in understanding the mechanisms of their biological functions. To identify the structures of sulfated oligosaccharides, we have developed HPLC map for the sulfated oligosaccharides. The HPLC mapping method facilitates structural analyses of *N*-glycans at cellular level. Therefore, we successfully collected sulfated oligosaccharides from LS12 cells derived from a human endothelial cell line by cotransfection with both *N*-acetylglucosamine-6-*O*-sulfotransferase-1 (GlcNAc6ST-1) and $\alpha 1,3$ -fucosyltransferase cDNAs.⁶⁰ p0180

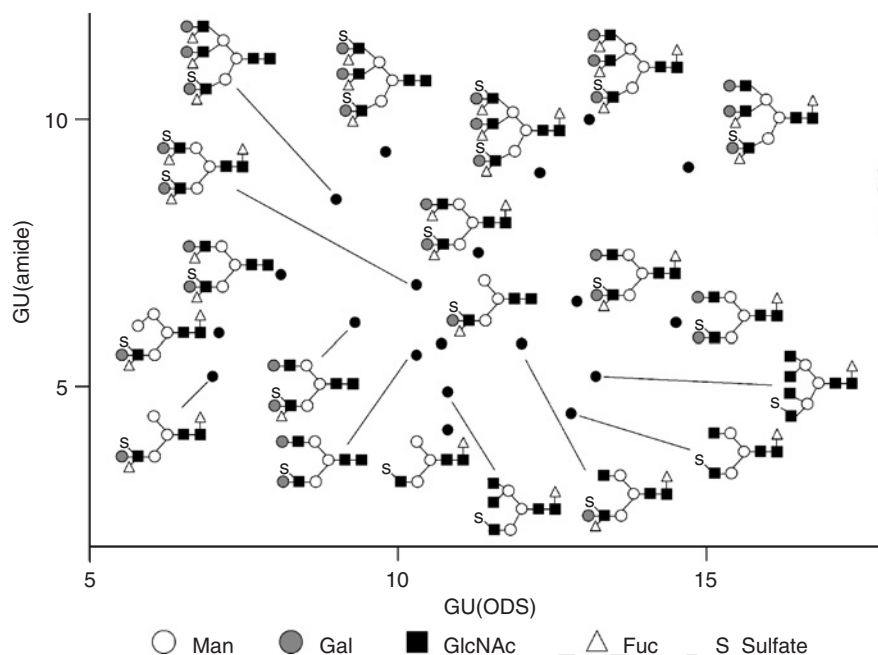


Figure 16 HPLC data of the desialylated sulfatooligosaccharides derived from LS12 cells.

f0080

The *N*-glycans were released from glycoprotein fractions of LS12 cells by glycoamidase A digestion and then labeled with 2-aminopyridine. The PA-oligosaccharide fractions were subjected to sialidase treatment so that we could focus on sulfated asialooligosaccharides as a first step of the collection of the HPLC data of sulfated glycans. The desialylated oligosaccharides were applied into DEAE column to fractionate anionic oligosaccharides. Then these anionic fractions were applied sequentially onto amide and ODS columns to isolate 21 anionic glycans, and their HPLC data were collected. MALDI-TOF-MS data indicated that all anionic oligosaccharides were sulfated. We characterized these oligosaccharides by various glycosidase treatments, desulfation reaction, and MALDI-TOF-MS analysis. Taking into account the substrate specificity of GlcNAc6ST-1, it was strongly suggested that sulfate groups at C-6 position of GlcNAc residues on the terminal *N*-acetylglucosamine sequence. In short, we elucidated the structures of 21 different sulfated oligosaccharides, which are bi-, tri-, and tetraantennary complex-type glycans sulfated at the C-6 position of *N*-acetylglucosamine residues (Figure 16). Furthermore, we identified 19 sulfated oligosaccharides resulting from various glycosidase treatments of the original sulfated oligosaccharides.

p0185

HPLC data of 40 kinds of sulfated oligosaccharides are now available to identify more promptly and effectively the structures of *N*-glycans including sulfated glycans.⁶¹

p0190

1.33.3.5 A Web Application, GALAXY

s0095

We also developed a Web application, GALAXY^{60,61} to utilize the accumulated 2/3-D map information more effectively.¹³ This application facilitates search of candidate structures corresponding the experimental data and enables us to predict coordinates of putative PA-glycans and to trace the effects of glycosidase treatments in a graphical manner.

p0195

1.33.3.6 A New Idea of HPLC Map Related to Microheterogeneity of *N*-Glycans

s0100

The utilization of the 2/3-D map information often leads to discovery of new oligosaccharides, which after thorough characterization will be added to the existing 2/3-D map data bank. Thus, the process continually enriches the 2/3-D data bank, and the richer the 2/3-D data bank, the more are the chances of finding unexpected oligosaccharide structures.

p0200

1.33.3.6.1 Application of parallelogram method to validate *N*-glycan structures on the 2-D map

N-glycan structures released from the same position's Asn residue on the same glycoprotein source are known to be microheterogeneous, sometimes differing only in a few monosaccharides. When a set of exoglycosidase digestion is performed, the GU values of the starting oligosaccharides and their derivatives tend to be at the nodes of a parallelogram in the 2-D map (Figure 17),^{50,54,57} because each monosaccharide is known to have its own specific unit contribution on both 2-D map axes.⁵⁴ Correctly identified structures from the same glycoprotein source validate each other by their closeness to the nodes of a parallelogram mesh. Therefore, this parallelogram method for mutual checking leads to the accurate identification of the sample structure.

s0105

p0205

1.33.3.6.2 Visual presentation of the *N*-glycan microheterogeneity

New visualization of known data can give us surprising new insights. We have so far analyzed many *N*-glycan structures, in each purified glycoprotein. At any Asn residue, we found not only one but several *N*-glycan structures, distributed on some characteristic area on the 2-D map (Figure 18). For example, *N*-glycans from Laccase (red circles) are closely arranged on the left side of the 2-D map, while *N*-glycans from human IgG (green circles) are closely arranged from the left side to the right side of the 2-D map. We call these HPLC data on the 2-D map microheterogeneity configurations, because they indicate the extent of each *N*-glycan's microheterogeneity. Several glycosyltransferases, which participate in *N*-glycan biosynthesis, might have gathered in each inner cell near the elongating sugar chain at that time. Therefore, each microheterogeneity configuration occupies only a limited, relatively small area, on the 2-D map. Our 2-D map can easily show each protein's specific area of microheterogeneity. These *N*-glycan microheterogeneity configurations resemble constellations in the galaxy.

s0110

p0210

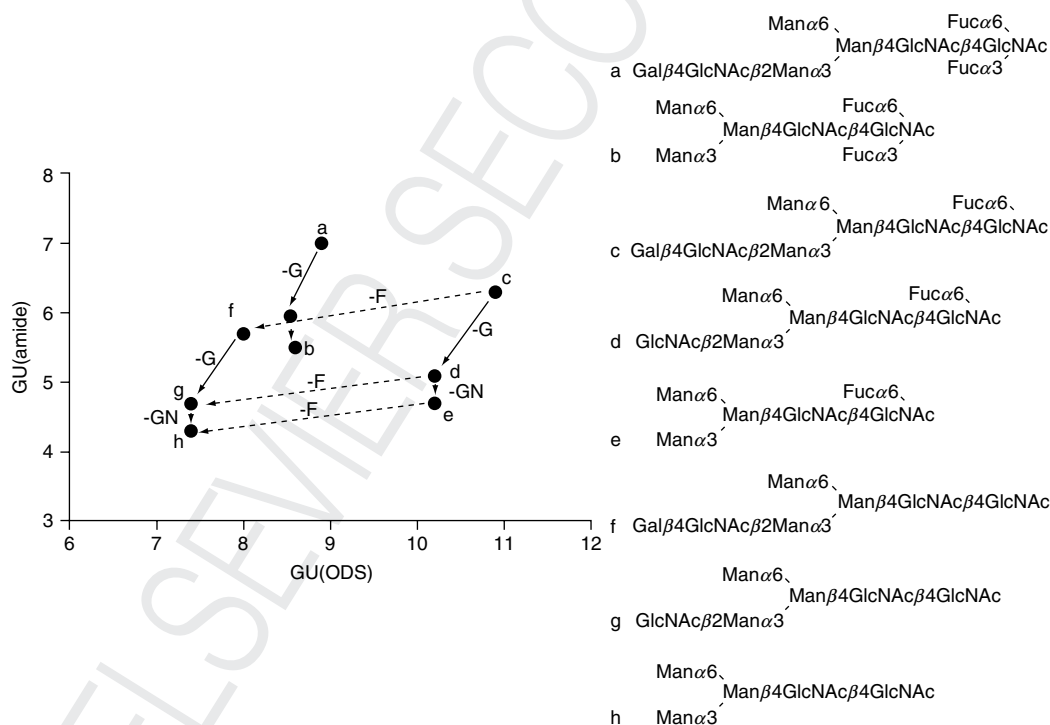


Figure 17 The parallelogram method to identify *N*-glycan structures on the HPLC map. The *N*-glycans were derived from human transferrin produced in *Trichoplusia ni* cells. Trajectories for α -fucosidase and β -galactosidase digestions are indicated by solid and dashed arrows, respectively. The short arrows (d-e and g-h) indicated the trajectories for β -*N*-acetylhexosaminidase digestion. F, fucose; G, galactose; GN, *N*-acetylhexosamine.

f0085

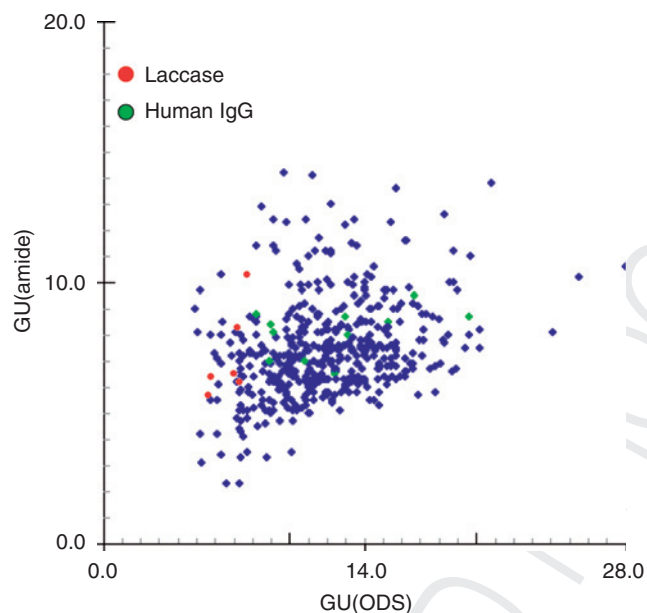


Figure 18 Visual representation of *N*-glycan microheterogeneity.

f0090

1.33.4 Summary

s0115

This chapter summarizes as follows:

p0215

1. Using three different HPLC columns, a mixture of neutral and sialyl oligosaccharides is completely separable.
2. The structural assignment of both neutral and sialyl *N*-linked oligosaccharides is very easy.
3. The database presented on the 3-D map is highly reproducible.
4. The sensitivity of PA-oligosaccharides detection is at pico- or femto-mol level.
5. This technique can easily lead to discovery of new structures, when the coordinates do not agree with those of any known compounds.

Acknowledgement

This work was supported by Grant-in-Aid for Scientific Research from the Ministry of Education, Culture, Sports, Science and Technology, and CREST of Japan Science and Technology Corporation.

p0220

Glossary

- Chlamydia trachomatis*** One of the most common causes of blindness and sexually transmitted diseases in humans. g0005
- erythropoietin** A protein that regulates the level of mammalian hematopoiesis, and is applied as a potential therapeutic reagent for anemia. The urinary erythropoietin (U-EPO) is purified from the urine of patients with aplastic anemia. U-EPO is a sialoglycoprotein with a molecular weight of 34000–39000 and possess three glycosylation sites (Asn-24,-38, and-83). g0010
- fibrinogen niigata $\alpha\beta$** A novel B β Asn-160 (TAA) to Ser (TGA) substitution identified in fibrinogen Niigata derived from a 64-year-old woman. The mutation creates an Asn-X-Ser-type glycosylation sequence, and a partially sialylated biantennary oligosaccharide is linked to the B β Asn-158 residue. g0015
- integrin $\alpha5\beta1$** The major fibronectin receptor recognizing the Arg-Gly-Asp sequence, and mediating fibronectin-dependent cell adhesion. g0020
- kallikrein(=kallidinogenase)** A serine protease that liberates lysyl-bradykinin, a vasoactive decapeptide, from kininogens. The complete amino acid sequence of kallikrein is reported and three *N*-glycosylation sites, Asn-78,-84, and -141, are identified. g0025
- mushroom lectin** A lectin from the fruiting body of the *Psathyrella velutina* mushroom (PVL) was found to bind specifically to *N*-acetylneuraminic acid, as well as to GlcNAc. g0030
- squid rhodopsin** Rhodopsin, the visual pigment in the photoreceptor cells, a typical seven transmembrane receptor. The *N*-terminal segment of rhodopsin is *N*-glycosylated. g0035

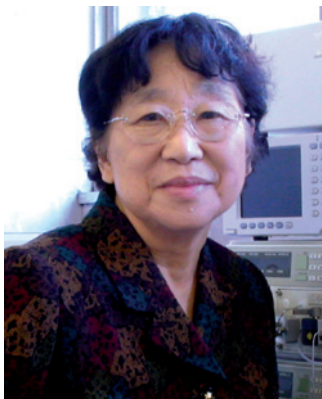
References

1. Takahashi, N. *Biochem. Biophys. Res. Commun.* **1977**, *76*, 1194–11201.
2. Takahashi, N.; Nishibe, H. *J. Biochem. (Tokyo)* **1978**, *84*, 1467–1473.
3. Takahashi, N.; Nishibe, H. *Biochim. Biophys. Acta* **1981**, *657*, 457–467.
4. Sugiyama, K.; Ishihara, H.; Tejima, S.; Takahashi, N. *Biochem. Biophys. Res. Commun.* **1983**, *112*, 155–160.
5. Elder, J. H.; Alexander, S. *Proc. Natl. Acad. Sci. U.S.A.* **1982**, *79*, 4540.
6. Plummer, T. H., Jr.; Elder, J. H.; Alexander, S.; Phelan, A. W.; Talentino, A. L. *J. Biol. Chem.* **1984**, *259*, 10700.
7. Yamamoto, S.; Hase, S.; Fukuda, S.; Sano, O.; Ikenaka, T. *J. Biochem.* **1989**, *105*, 547–555.
8. Nakagawa, H.; Kawamura, Y.; Kato, K.; Shimada, I.; Arata, Y.; Takahashi, N. *Anal. Biochem.* **1995**, *226*, 130–138.
9. Takahashi, N.; Nakagawa, H.; Fujikawa, K.; Kawamura, Y.; Tomiya, N. *Anal. Biochem.* **1995**, *226*, 139–146.
10. GALAXY. Glycoanalysis by the three axes of MS and chromatography. Website: <http://www.glycoanalysis.info>.
11. Tomiya, N.; Awaya, J.; Kurono, M.; Endo, S.; Arata, Y.; Takahashi, N. *Anal. Biochem.* **1988**, *171*, 73–90.
12. Lund, J.; Takahashi, N.; Pound, J. D.; Goodall, M.; Nakagawa, H.; Jefferis, R. *Faseb. J.* **1995**, *9*, 115–119.
13. Takahashi, N.; Kato, K. *Trends Glycosci. Glycotech.* **2003**, *15*, 235–251.
14. Tsuda, E.; Goto, M.; Murakami, A.; Akai, K.; Ueda, M.; Kawanishi, G.; Takahashi, N.; Sasaki, R.; Chiba, H.; Ishihara, H., et al. *Biochemistry* **1988**, *27*, 5646–5654.
15. Tomiya, N.; Yamaguchi, T.; Awaya, J.; Kurono, M.; Endo, S.; Arata, Y.; Ishihara, H.; Mori, M.; Tejima, S.; Takahashi, N. *Biochemistry* **1988**, *27*, 7146–7154.
16. Takahashi, N.; Ishii, I.; Ishihara, H.; Mori, M.; Tejima, S.; Jefferis, R.; Endo, S.; Arata, Y. *Biochemistry* **1987**, *26*, 1137–1144.
17. Yamazumi, K.; Shimura, K.; Terukina, S.; Takahashi, N.; Matsuda, M. *J. Clin. Invest.* **1989**, *83*, 1590–1597.
18. Takahashi, N.; Hitotsuya, H.; Hanzawa, H.; Arata, Y.; Kurihara, Y. *J. Biol. Chem.* **1990**, *265*, 7793–7798.
19. Lund, J.; Tanaka, T.; Takahashi, N.; Sarmay, G.; Arata, Y.; Jefferis, R. *Mol. Immunol.* **1990**, *27*, 1145–1153.
20. Hayashi, M.; Tsuru, A.; Mitsui, T.; Takahashi, N.; Hanzawa, H.; Arata, Y.; Akazawa, T. *Eur. J. Biochem.* **1990**, *191*, 287–295.
21. Maekawa, H.; Yamazumi, K.; Muramatsu, S.; Kaneko, M.; Hirata, H.; Takahashi, N.; De Bosch, N. B.; Carvajal, Z.; Ojeda, A.; et al. *J. Biol. Chem.* **1991**, *266*, 11575–11581.
22. Yoshida, T.; Takahashi, N.; Nakashima, I. *Mol. Immunol.* **1991**, *28*, 1121–1130.
23. Tezuka, K.; Hayashi, M.; Ishihara, H.; Akazawa, T.; Takahashi, N. *Eur. J. Biochem.* **1992**, *203*, 401–413.
24. Shoji, H.; Takahashi, N.; Nomoto, H.; Ishikawa, M.; Shimada, I.; Arata, Y.; Hayashi, K. *Eur. J. Biochem.* **1992**, *207*, 631–641.
25. Maekawa, H.; Yamazumi, K.; Muramatsu, S.; Kaneko, M.; Hirata, H.; Takahashi, N.; Arocha-Pinango, C. L.; Rodriguez, S.; Nagy, H. *J. Clin. Invest.* **1992**, *90*, 67–76.
26. Tomiya, N.; Awaya, J.; Kurono, M.; Hanzawa, H.; Shimada, I.; Arata, Y.; Yoshida, T.; Takahashi, N. *J. Biol. Chem.* **1993**, *268*, 113–126.
27. Nakagawa, H.; Takahashi, N.; Fujikawa, K.; Kawamura, Y.; Iino, M.; Takeya, H.; Ogawa, H.; Suzuki, K. *Glycoconj. J.* **1995**, *12*, 173–181.
28. Nakagawa, H.; Zheng, M.; Hakomori, S.; Tsukamoto, Y.; Kawamura, Y.; Takahashi, N. *Eur. J. Biochem.* **1996**, *237*, 76–85.
29. Ohsuga, H.; Su, S.-N.; Takahashi, N.; Yang, S.-Y.; Nakagawa, H.; Shimada, I.; Arata, Y.; Lee, Y. C. *J. Biol. Chem.* **1996**, *271*, 26653–26658.
30. Lund, J.; Takahashi, N.; Pound, J. D.; Goodall, M.; Jefferis, R. *J. Immunol.* **1996**, *157*, 4963–4969.
31. Kuo, C.; Takahashi, N.; Swanson, A. F.; Ozeki, Y.; Hakomori, S. *J. Clin. Invest.* **1996**, *98*, 2813–2818.
32. Kibe, T.; Fujimoto, S.; Ishida, C.; Togari, H.; Wada, Y.; Okada, S.; Nakagawa, H.; Tsukamoto, Y.; Takahashi, N. *J. Clin. Biochem. Nutr.* **1996**, *21*, 57–63.
33. Yamada, E.; Tsukamoto, Y.; Sasaki, R.; Yagyu, K.; Takahashi, N. *Glycoconj. J.* **1997**, *14*, 401–405.
34. Takahashi, N.; Lee, K. B.; Nakagawa, H.; Tsukamoto, Y.; Masuda, K.; Lee, Y. C. *Anal. Biochem.* **1998**, *255*, 183–187.
35. Farooq, M.; Takahashi, N.; Drayson, M.; Lund, J.; Jefferis, R. *Adv. Exp. Med. Biol.* **1998**, *435*, 95–103.
36. Routier, F. H.; Hounsell, E. F.; Rudd, P. M.; Takahashi, N.; Bond, A.; Hay, F. C.; Alavi, A.; Axford, J. S.; Jefferis, R. *J. Immunol. Methods* **1998**, *213*, 113–130.
37. Takahashi, N.; Yamada, W.; Masuda, K.; Araki, H.; Tsukamoto, Y.; Galinha, A.; Sautès, C.; Kato, K.; Shimada, I. *Glycoconj. J.* **1998**, *15*, 905–914.
38. Mukofujiwara, Y.; Otsuka, T.; Waguri, Y.; Matsui, N.; Asai, K.; Kato, T.; Araki, H.; Tsukamoto, Y.; Takahashi, N. *J. Clin. Biochem. Nutr.* **1998**, *25*, 131–142.
39. Sugo, T.; Nakamikawa, C.; Takano, H.; Mimuro, J.; Yamaguchi, S.; Mosesson, M. W.; Meh, D. A.; DiOrio, J. P.; Takahashi, N.; Takahashi, H.; Nagai, K.; Matsuda, M. *Blood* **1999**, *94*, 3806–3813.
40. Takahashi, N.; Tsukamoto, Y.; Shiosaka, S.; Kishi, T.; Hakoshima, T.; Arata, Y.; Yamaguchi, Y.; Kato, K.; Shimada, I. *Glycoconj. J.* **1999**, *16*, 405–414.
41. Masuda, K.; Takahashi, N.; Tsukamoto, Y.; Honma, H.; Kohri, K. *Biochem. Biophys. Res. Commun.* **2000**, *268*, 814–817.
42. Ailor, E.; Takahashi, N.; Tsukamoto, Y.; Masuda, K.; Rahman, B. A.; Jarvis, D. L.; Lee, Y. C.; Betenbaugh, M. J. *Glycobiology* **2000**, *10*, 837–847.
43. Lund, J.; Takahashi, N.; Popplewell, A.; Goodall, M.; Pound, J. D.; Tyler, R.; King, D. J.; Jefferis, R. *Eur. J. Biochem.* **2000**, *267*, 7246–7256.
44. Hashimoto, S.; Hashimoto, M.; Yanai, M.; Kumasaka, K.; Kawano, K.; Senou, A.; Araki, H.; Tsukamoto, Y.; Takahashi, N. *J. Clin. Biochem. Nutr.* **2000**, *28*, 81–89.
45. Takahashi, N.; Khoo, K.-H.; Suzuki, N.; Johnson, J. R.; Lee, Y. C. *J. Biol. Chem.* **2001**, *276*, 23230–23239.
46. Ueda, H.; Matsumoto, H.; Takahashi, N.; Ogawa, H. *J. Biol. Chem.* **2002**, *277*, 24916–24925.
47. Takahashi, N.; Cohen-Solal, J.; Galinha, A.; Fridman, W. H.; Sautes-Fridman, C.; Kato, K. *Glycobiology* **2002**, *12*, 507–515.
48. Holland, M.; Takada, K.; Okumoto, T.; Takahashi, N.; Kato, K.; Adu, D.; Ben-Smith, A.; Harper, L.; Savage, C. O.; Jefferis, R. *Clin. Exp. Immunol.* **2002**, *129*, 183–190.
49. Nagaya, M.; Kobayashi, J.; Takahashi, N.; Kato, K.; Yoshimura, T. *J. Insect Biotech. Sericol.* **2003**, *72*, 79–86.
50. Takahashi, N.; Masuda, K.; Hiraki, K.; Yoshihara, K.; Huang, H. H.; Khoo, K. H.; Kato, K. *Eur. J. Biochem.* **2003**, *270*, 2627–2632.
51. Wojczyk, B. S.; Takahashi, N.; Levy, M. T.; Andrews, D. W.; Abrams, W. R.; Wunner, W. H.; Spitalnik, S. L. *Glycobiology* **2005**, *15*, 655–666.
52. Lee, Y. C.; Lee, B. I.; Tomiya, N.; Takahashi, N. *Anal. Biochem.* **1990**, *188*, 259–266.
53. Tomiya, N.; Lee, Y. C.; Yoshida, T.; Wada, Y.; Awaya, J.; Kurono, M.; Takahashi, N. *Anal. Biochem.* **1991**, *193*, 90–100.
54. Tomiya, N.; Takahashi, N. *Anal. Biochem.* **1998**, *264*, 204–210.
55. Lee, Y. C.; Lee, B. I.; Tomiya, N.; Takahashi, N. *Anal. Biochem.* **1990**, *188*, 259–266.
56. Nakagawa, H.; Kawamura, Y.; Kato, K.; Shimada, I.; Arata, Y.; Takahashi, N. *Anal. Biochem.* **1995**, *226*, 130–138.

57. Rosen, S. D. *Am. J. Pathol.* **1999**, *155*, 1013–1020.
58. Fiete, D.; Srivastava, V.; Hindsgaul, O.; Baenziger, J. U. *Cell* **1991**, *67*, 1103–1110.
59. Martini, R.; Xin, Y.; Schmitz, B.; Schachner, M. *Eur. J. Neurosci.* **1992**, *4*, 628–639.
60. Kimura, N.; Mitsuoka, C.; Kanamori, A.; Hiraiwa, N.; Uchimura, K.; Muramatsu, T.; Tamatani, T.; Kansas, G. S.; Kannagi, R. *Proc. Natl. Acad. Sci. USA* **1999**, *96*, 4530–4535.
61. Yagi, H.; Takahashi, N.; Yamaguchi, Y.; Kimura, N.; Uchimura, K.; Kannagi, R.; Kato, K. *Glycobiology* **2005**, *15*, 1051–1060.

ELSEVIER SECOND PROOF

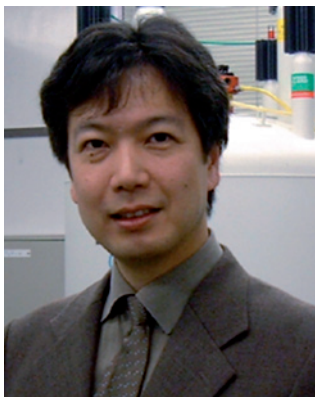
Biographical Sketch



Noriko Takahashi, Ph.D., is Visiting Professor of Graduate School of Pharmaceutical Sciences at the Nagoya City University, Nagoya Japan. She graduated in 1951 from the Faculty of Technology, Nagoya University, and obtained her Ph.D. in 1960 from the Faculty of Science, Nagoya University. She served as an Assistant Professor, an Associate Professor and a Professor at Nagoya City University Medical School and College of Nursing from 1966 to 1992; and as a Director of GlycoLab at the Central Research Institute of Nakano Vinegar Co. Ltd. from 1992 to 2000. She is Visiting Professor of Graduate School of Pharmaceutical Sciences at the Nagoya City University, from 2000 to 2005. She assumed her present position in 2005. She is a member of the Japanese Chemical Society, the Japanese Biochemical Society, the Japanese Society of Carbohydrate Research, and the Society for Glycobiology (USA). She has been the recipient of many research grants from the Japanese Ministry of Education Culture Sports Science and Technology; and private industries. She has published more than 135 research papers and has been the author and editor of several books. She received the academic honor "The membership in the Johns Hopkins Society of Scholars" in 1997.



Hirokazu Yagi, is postgraduate student of the Graduate School of Pharmaceutical Sciences at the Nagoya City University, Nagoya Japan. He graduated in 2002 from the Faculty of Pharmaceutical Sciences, Nagoya City University. His current major research interest is the structural functional relationship between glycans and proteins in cell surface.



Koichi Kato received his Ph.D. in 1991 at Grad. Sch. of Pharmaceutical Sciences, the University of Tokyo (Prof. Yoji Arata), and continued his research as an Assistant Professor and then as a Lecturer in the same group. In 2000 he received the Award for Young Scientists of the Pharmaceutical Society of Japan and moved to his current position at Nagoya City University. His research interests include development of NMR and HPLC mapping techniques for structural analyses of glycoproteins. His group has developed GALAXY (<http://www.glycoanalysis.info/ENG/index.html>), a web application for identification of *N*-linked oligosaccharides. Since 2004 he has been holding posts concurrently in Institute for Molecular Science and in GLYENCE, a company to exploit glycotechnology of his group.

Non-Print ItemsAuthor Contact Information:

Noriko Takahashi
Graduate School of Pharmaceutical Sciences
Nagoya City University
3-1 Tanabe-dori, Mizuho-ku
Nagoya 467-8603
Japan
81 52 836 3447
81 52 836 3447
ntakahas@phar.nagoya-cu.ac.jp

Hirokazu Yagi
Graduate School of Pharmaceutical Sciences
Nagoya City University
3-1 Tanabe-dori, Mizuho-ku
Nagoya 467-8603
Japan
81 52 836 3450
p92049@phar.nagoya-cu.ac.jp

Koichi Kato
Graduate School of Pharmaceutical Sciences
Nagoya City University
3-1 Tanabe-dori, Mizuho-ku
Nagoya 467-8603
Japan
81 52 836 3450
81 52 836 3450
kkato@phar.nagoya-cu.ac.jp

Abstract:

The two-/three-dimensional mapping method, which has been developed for the structural determination of asparagine-linked oligosaccharides (*N*-glycans) in glycoproteins, is summarized in this chapter.

In this method, *N*-glycans are released from the protein portion by glycoamidase A digestion and the reducing ends are fluorescence labeled with 2-aminopyridine. These pyridylamino (PA)-glycans are separated by high-performance liquid chromatography (HPLC) using three different columns sequentially, and from the elution positions on three HPLC columns, the structures of PA-glycans are simultaneously estimated.

The structure of a sample PA-glycan can be estimated by comparing its elution position on the map with the positions of the known reference *N*-glycans plotted on the 2-D map. The sample PA-glycan and one of the candidate reference PA-glycans are co-injected into two HPLC columns to confirm coincidence of the peak position. Furthermore, the sample PA-glycans are digested with several glycosidases, then the changes in the elution positions are again compared with those of the reference *N*-glycans.

This method is useful not only as an analytical procedure for *N*-glycan structures, but also as a means of isolating large-scale samples for NMR spectroscopy or MS spectrometry. Approximately 1 mg of glycoprotein is used for the method. PA-oligosaccharides (pico-mols or femto-mols) are used for one run of HPLC analysis.

Keywords: Amide-silica column; DEAE column; GALAXY; Glycoamidase A; HPLC map; HPLC mapping method; Microheterogeneity; *N*-glycan structures; *N*-glycosylation profile; ODS column/ PA-glycans;/ Structural analysis